

A. BIGOS\*, E. BEŁTOWSKA-LEHMAN\*, P. INDYKA\*\*, M. J. SZCZERBA\*, M. KOT\*\*\*, M. GROBELNY\*\*\*\*

## ELECTRODEPOSITION AND PROPERTIES OF NANOCRYSTALLINE Ni-BASED ALLOYS WITH REFRACTORY METAL FROM CITRATE BATHS

### ELEKTROOSADZANIE I WŁAŚCIWOŚCI NANOKRYSTALICZNYCH STOPÓW NA OSNOWIE NIKLU Z TRUDNOTOPLIWYM METALEM Z KĄPIELI CYTRYNIANOWYCH

The main aim of the present work was to determine the optimal conditions for electrodeposition of metallic Ni-Mo coatings of enhanced micromechanical properties. These alloys were electrodeposited on the ferritic steel substrate, under galvanostatic regime in a system with a rotating disk electrode (RDE), from an aqueous citrate complex solution containing nickel and molybdenum salts. The effect of the electrolyte solution pH (adjusted by sulphuric acid or ammonia) on the molybdenum content and on deposit quality as well as on the current efficiency of the electrodeposition process, has been studied. It was established that increase of bath pH is correlated with gradual increase of molybdenum content in deposits up to pH 7, where the maximum concentration of Mo(VI) electroactive citrate complex ions  $[\text{MoO}_4(\text{Cit})\text{H}]^{4-}$  (Cit=  $\text{C}_6\text{H}_5\text{O}_7^{3-}$ ) in plating bath was observed. In the selected bath of the optimum pH value, the effect of cathodic current density, as a crucial operating parameter which strongly controls the chemical composition and microstructure parameters (e.g. phase compositions, crystallite size), on the mechanical and tribological properties of the resulting coatings has been determined. It has been shown that – under all investigated current density range – crack-free, well adherent Ni-Mo coatings, characterized by microhardness of 6.5-7.8 GPa, were obtained. Alloys deposited at higher tested current densities (above  $3.5 \text{ A/dm}^2$ ) were characterized by compact and uniform microstructure, and thus had the highest wear and friction resistance.

*Keywords:* Ni-Mo coatings, citrate baths, induced co-deposition, mechanical properties

Głównym celem pracy było ustalenie optymalnych warunków procesu elektroosadzania metalicznych powłok Ni-Mo o podwyższonych właściwościach mikromechanicznych. Charakteryzowane stopy zostały osadzone na podłożu ze stali ferrytycznej, w warunkach galwanostaticznych, w modelowym układzie z wirującą elektrodą dyskową (WED), z wodnych kompleksowych roztworów cytrynianowych zawierających sole niklu i molibdenu. Określono wpływ pH elektrolitu (regulowanego przez dodatek kwasu siarkowego lub amoniaku) na zawartość molibdenu w stopie, jakość osadów, jak również wydajność prądową procesu elektroosadzania. Stwierdzono, że wzrost pH jest związany ze stopniowym zwiększaniem zawartości molibdenu w powłokach. Maksymalną zawartość molibdenu uzyskano w stopach wydzielonych z kąpeli galwanicznej o pH 7, gdzie jednocześnie zaobserwowano najwyższe stężenie cytrynianowych, elektroaktywnych kompleksów molibdenu typu  $[\text{MoO}_4(\text{Cit})\text{H}]^{4-}$  (Cit=  $\text{C}_6\text{H}_5\text{O}_7^{3-}$ ). Dla wybranej kąpeli galwanicznej o optymalnym pH badano wpływ gęstości prądu katodowego (kluczowego parametru operacyjnego, kontrolującego między innymi skład chemiczny oraz mikrostrukturę, w tym skład fazowy i rozmiar krystalitów) na właściwości mechaniczne i tribologiczne wytworzonych powłok. Wykazano, że w całym analizowanym zakresie gęstości prądu, otrzymano powłoki Ni-Mo bez siatki mikropełnięć, o dobrej adhezji do stalowego podłoża, charakteryzujące się podwyższoną twardością w zakresie 6.5 do 7.8 GPa. Ponadto, powłoki osadzone przy wyższych gęstościach prądu (powyżej  $3.5 \text{ A/dm}^2$ ) odznaczają się zwartą i jednorodną mikrostrukturą, a tym samym najwyższą odpornością na zużycie przez tarcie.

### 1. Introduction

Electrodeposited hard chromium coatings have been used extensively in many industries as protective, anticorrosion coatings and decorative finishes. Despite excellent properties and low manufacturing costs, the electrolyte solution used for their preparation contains toxic hexavalent Cr(VI) ions and according to EU directives (2000/53/WE, 2011/37/UE) have to

be eliminated [1]. Due to this reason, extensive research to find chromium alternatives has been undertaken. Promising substitutes for chromium could be nickel-based alloys containing refractory metal (such as Ni-Mo), which are characterized by high hardness, high wear, thermal and corrosion resistances as well as catalytic activity for hydrogen evolution [2-3]. Despite the interesting physico-chemical properties these alloys are difficult to obtain by conventional thermal methods due to the

\* POLISH ACADEMY OF SCIENCES, INSTITUTE OF METALLURGY AND MATERIALS SCIENCE, KRAKOW, POLAND

\*\* FACULTY OF CHEMISTRY, JAGIELLONIAN UNIVERSITY, KRAKOW, POLAND

\*\*\* AGH UNIVERSITY OF SCIENCE AND TECHNOLOGY, KRAKOW, POLAND

\*\*\*\* MOTOR TRANSPORT INSTITUTE, WARSZAWA, POLAND

large difference in metal melting points (Ni – 1455°C, Mo – 2620°C) and their limited mutual solubility. Convenient way to produce these type of coatings, which overcomes above mentioned problems, is a low-temperature and relatively simple electrodeposition technique. It enables uniform surface covering with simultaneous control of thickness, microstructure and thus allows to influence the properties of the layer. Moreover, the electrodeposition processes take place in aqueous solutions at relatively low temperatures (below 100°C).

Most of published papers were devoted to the preparation of Ni-Mo coating for the hydrogen electrode with good catalytic properties in alkaline solution [3-5]. However, these coatings of good quality (crack-free, non-porous, of a good adhesion to the substrate) are difficult to produce by electrodeposition technique [6-7]. Thus in the literature of the subject, not much attention is paid to their mechanical properties, important for protective materials, e.g. in the automotive and aviation industries [8-9].

It is known, that molybdenum in metallic state cannot be separately electrodeposited from aqueous solutions of its ions, but it can be co-deposited with iron-group metals (such as Ni, which acts as a catalyst) with an alloy formation. This phenomenon was called induced co-deposition by Brenner, who concluded that during electrodeposition process the observed transfer of the polarization energy of the inducing metal (iron group metals) to molybdenum results in its co-discharge [10]. The mechanism is still not clearly understood, although a few hypotheses were presented in the literature [11-16]. Most of them refer to the possibility of a multi-step reduction of some molybdenum species. Among others, a surface adsorbed intermediate mechanism has been recently proposed [12-13]. Some authors have suggested that at first the molybdate is electrochemically reduced to molybdenum oxide, and subsequently undergoes a chemical reduction by atomic hydrogen previously adsorbed on the inducing metal [14-16].

It was found that from solution containing only molybdenum and nickel ions, it is impossible to obtain alloys with more than 2 wt.% of molybdenum. The electrodeposits of this kind are of poor quality and contain high amount of molybdenum oxides, what is probably related to the formation of multimolecular heteropolymolybdates, which are difficult to electrodepose. After addition of an appropriate complexing agent into such solution (e.g. sodium citrate), heteropolymolybdates are decomposed and at first the formation of the electrochemically active molybdenum  $[\text{MoO}_4(\text{Cit})\text{H}]^{4-}$  and then nickel  $[\text{NiCit}]^-$  citrate complexes is observed [17].

Furthermore, aqueous solution containing sodium citrate is characterized by buffering, leveling and brightening properties [18]. In the designed electroplating bath, essential is to maintain an appropriate balance between its components. It was found that in the analyzed system good quality coatings are obtained when the concentration of citrate ions is slightly higher than the total concentration of the metal ions in solution and also when the concentration of Ni(II) is significantly higher than for Mo(VI) ions [19].

In the presented study, Ni-Mo alloys were electrodeposited from environmentally friendly citrate electrolyte solution of previously determined optimal concentration ratio of reagents [19]. The influence of pH bath and current density on chemi-

cal composition, microstructure and mechanical properties of electrodeposited Ni-Mo alloys were investigated.

## 2. Experimental

The binary Ni-Mo alloys were electrochemically deposited from aqueous solutions containing analytical grade purity chemicals: 0.2M NiSO<sub>4</sub>, 0.006M Na<sub>2</sub>MoO<sub>4</sub> and 0.3M Na<sub>3</sub>C<sub>6</sub>H<sub>5</sub>O<sub>7</sub> of pH in the range from 4 to 10 adjusted by an addition of sulphuric acid or ammonia. No brighteners, detergents and wetting agents were used. The electroplating was conducted in the galvanostatic (in the range of current density from 0.5 to 5 A/dm<sup>2</sup>) or potentiostatic conditions, in a system with a rotating (at 640 rpm) disk electrode (RDE), at room temperature. As a cathode low carbon steel disks (~0.028 dm<sup>2</sup>) were used, which (prior to electrodeposition) were chemically polished in the solution of hydrogen peroxide and oxalic acid. For the anode a platinum wire (~0.5 dm<sup>2</sup>) was used. Electrochemical measurements of the Ni-Mo deposition process were performed in potentiostatic conditions using potentiostat/galvanostat PAR 273A, where the cathode potentials were referred to the saturated calomel electrode (SCE). The steady-state partial polarization curves were calculated from the quantities of electric charge as well as from the mass and chemical composition of samples deposited at various cathode potentials along the global polarization curve. For those investigations the chemical composition and mass of the deposits were determined by the atomic absorption spectroscopy using spectrophotometer UNICAM SP-90. In other experiments, the chemical composition was also analyzed by energy dispersive X-ray spectroscopy from cross-section of the samples and a mean value was calculated from a minimum of six measurements [20]. The calculations of equilibrium composition of the analyzed electrolyte solution were done by Hyperquad Simulation and Speciation program (HySS2009) [21]. The data referring to equilibrium constants adopted in the calculations were taken from [22-23]. The surface and cross-section morphologies of coatings were examined by scanning electron microscopy (ESEM FEI XL-30). X-ray diffraction technique (Bruker D8 Discover) was used to determine phase composition and an average grain size of deposits. High resolution XPS spectra of the molybdenum oxides were collected using an ESCA 150 spectrometer (VSW Scientific Instruments Ltd., Manchester, England) equipped with an aluminum K $\alpha$  (1486.6 eV, 200W) radiation source. The corrosion behavior of chosen coatings was evaluated by potentiodynamic polarization measurements in 0.5M NaCl and 0.5M Na<sub>2</sub>SO<sub>4</sub> solutions (the scan rate: 1 mV/s, the potential range: -150mV to +1500 mV). The AUTOLAB PGSTAT302N potentiostat/galvanostat with General Purpose Electrochemical System (GPES) software was used to control the experiment as well as for collecting and analyzing data. A three-electrode system with the following electrodes: working electrode (electrodeposited on steel substrate Ni-Mo (5.4 wt.% Mo) and chromium (WSK PLZ Rzeszow) coatings as well as S235JR steel samples), the reference electrode (silver chloride electrode) and the counter electrode (platinum wire) was used. The value of microhardness and Young's modulus were measured during indentation test with a Vickers diamond indenter according to ISO 14577-1 stan-

dard (Micro-Combo-Tester, CSEM Instrument). Friction and wear resistance properties of Ni-Mo alloys were determined by ball-on-disk tests performed under constant rotating speed of 60 rpm and load of 1N (ISO 20808, ASTM G99-05 standards). The surface roughness ( $R_a$  – the average roughness parameter) of Ni-Mo coatings was determined by profilometer (TOPO 01P), which was used to obtain 3D images from the sample surfaces of  $1.25 \times 1.25$  mm.

### 3. Results

The electroplating process of alloy coatings is generally affected by the type of galvanic bath and operating parameters, among which the cathodic current density ( $j$ ) is the most important factor. On the other hand, the pH value is the most significant parameter for complex plating bath with a fixed composition. Hence, in the present study the impact of both parameters (pH,  $j$ ) on electrodeposition process of Ni-Mo coatings was considered.

The influence of pH value on molybdenum content in Ni-Mo alloys electrodeposited galvanostatically at current density of  $2.5 \text{ A/dm}^2$  and on the calculated concentration of electroactive Mo(VI) citrate complexes of the type  $[\text{MoO}_4(\text{Cit})\text{H}]^{4-}$  (Cit =  $\text{C}_6\text{H}_5\text{O}_7^{3-}$ ) in the electrolyte solution are shown in Fig. 1.

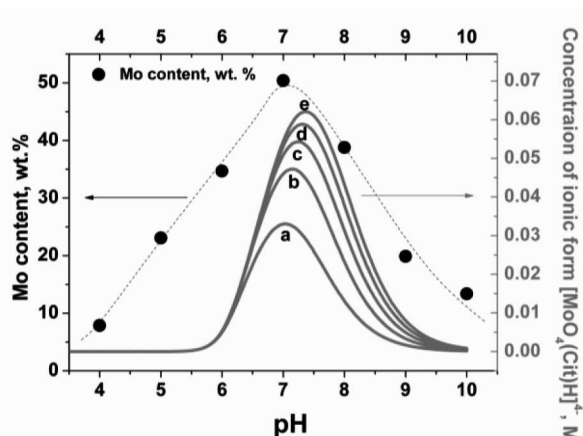


Fig. 1. Molybdenum content in Ni-Mo alloys electrodeposited at  $j = 2.5 \text{ A/dm}^2$  and concentration of the electroactive molybdenum species  $[\text{MoO}_4(\text{Cit})\text{H}]^{4-}$  in solution, calculated for the following molar ratio  $[\text{Mo(VI)}]:[\text{Cit}]$ : a) 1:1, b) 1:2, c) 1:3, d) 1:4, e) 1:5 as a function of pH (Cit =  $\text{C}_6\text{H}_5\text{O}_7^{3-}$ )

As seen, an increase of bath pH is distinctly correlated with gradual increase of the molybdenum content in Ni-Mo deposits up to about pH 7, where the maximum concentration of Mo(VI) electroactive citrate complex ions in plating bath was observed. On the other hand, further increase of the pH value beyond 7 causes a significant decrease of the molybdenum content of the alloy. This dependence has strong influence on the deposit quality and corresponds to changes of surface morphology of the obtained coatings from non-uniform with visible cracks to a more compact and crack-free surface.

It was found that Ni-Mo coatings of the best quality were deposited with the highest current efficiency from electrolyte solutions of pH above 8 (Fig. 2 and Fig. 3). As seen in Fig. 3,

electrodeposition process was the most efficient in the electrolyte solution of pH 10 (about 80%). However, in order to achieve this pH value an addition of a significant amount of ammonia was necessary. Due to this reason, bath of pH 9 (as the optimal) was chosen for further investigation of the kinetics of Ni-Mo electrodeposition process.

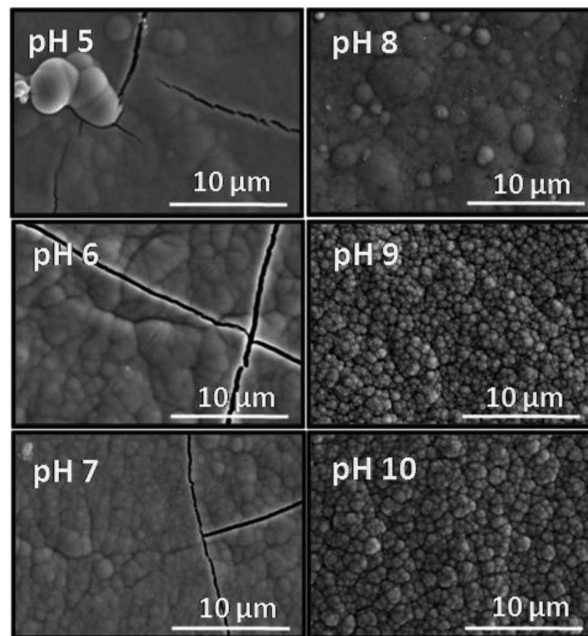


Fig. 2. SEM images of surface morphology of Ni-Mo coatings ( $\sim 10 \mu\text{m}$ ) electrodeposited from electrolytic baths of pH in the range of 5-10 and at current density of  $2.5 \text{ A/dm}^2$

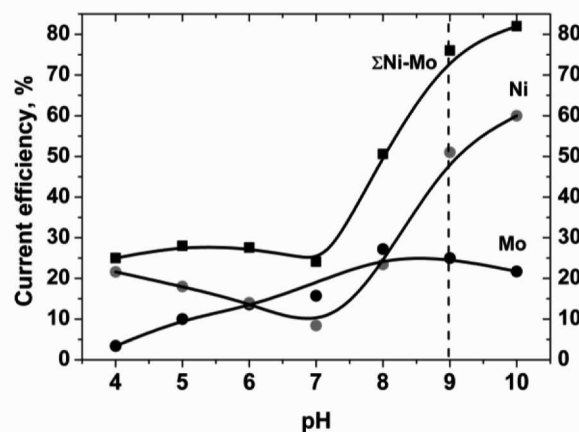


Fig. 3. Current efficiency of Ni-Mo electrodeposition process at current density of  $2.5 \text{ A/dm}^2$  (total and partial) as a function of the pH value of electrolyte solution

During electrochemical process of Ni-Mo alloy deposition, at least three main reactions occur simultaneously at the cathode: Ni(II) and Mo(VI) species electroreduction and hydrogen evolution. Therefore, in order to characterize the process of Mo(VI) and Ni(II) co-discharge, the method of resolving the total polarization curve of alloy electrodeposition into partial polarization curves (for deposition of alloy components) was applied. This procedure allows to determine the rate of the deposition of parent metals and the rate of hydrogen evolution. The corresponding value for hydrogen evolution (assumption the only side reaction) was calculat-

ed from the difference between the total charge and quality of electrical charges consumed for deposition of metals [24]. Figure 4 shows the total and partial polarisation curves for Ni-Mo deposition determined in the electrolyte solution of pH 9, at chosen hydrodynamic condition (corresponding to the disk rotating speed of 640 rpm).

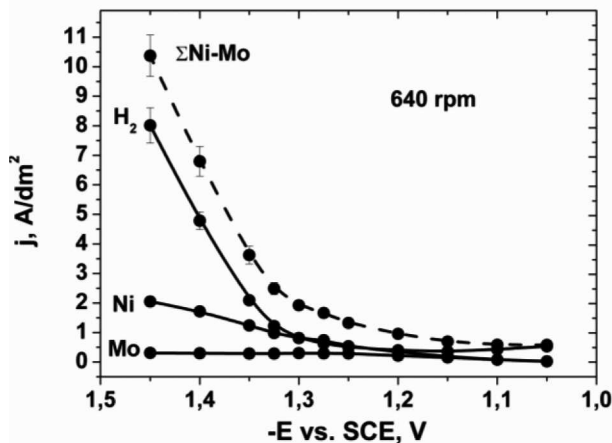


Fig. 4. Global and partial polarization curves recorded during Ni-Mo deposition under potentiostatic condition at 640 rpm

As seen from the data presented in Figure 4, the partial current density of molybdenum deposition is practically independent of the cathode potential, thus the mass transport is a stage of the process which controls Mo(VI) species discharge at the cathode (molybdenum is deposited into the alloy at a limiting diffusion current). This result was also confirmed by studies performed under different hydrodynamic conditions [19]. On the other hand, Ni(II) species undergo electroreduction with activation control (charge transfer reaction is the slowest step of the process). These effects have resulted in a decrease of the relative content of molybdenum in the alloy with an increase of current density (or cathode potential decrease). Also, during co-deposition process a significant increase of the hydrogen evolution is observed due to the low hydrogen overvoltage on the molybdenum oxides or on molybdenum alloys [25-26]. Furthermore, on the basis of SEM, XRD and XPS analysis of resulting deposits, it was found that metallic, nanocrystalline and homogenous coatings are obtained when the potential is shifted to more negative values than  $-1.35\text{V/SCE}$ . In contrary, when the less negative potential is applied, at the cathode molybdenum oxides dominate. These observations support the hypothesis that the first stage of the induced Ni-Mo codeposition is an incomplete electroreduction of Mo(VI) species to molybdenum oxides (Fig. 5). Moreover, the obtained results rather exclude the opinion of the reduction of molybdenum oxides by atomic hydrogen, because in the range of the cathode potential, where molybdenum oxides are formed, hydrogen evolution is the dominant process (Fig. 4).

In the electroplating technique, the cathodic current density is a crucial parameter which determines chemical composition, microstructure, and hence the mechanical properties of obtained coatings. Due to this reason, in order to characterize Ni-Mo coatings, electrodeposition was carried out galvanostatically in the range of the current density from  $0.5$  to  $5\text{ A/dm}^2$ , at the RDE speed of  $640\text{ rpm}$ . It was established that a significant decrease of the molybdenum content from about

$20$  to about  $5\text{ wt.}\%$  with the current density increase from  $0.5$  to  $5\text{ A/dm}^2$  has occurred (Fig. 6). These results are in close agreement with data reported in numerous papers [7-8, 26]. Moreover, an increase in the rate of mass transport causes reduction of the current efficiency related to the higher content of (diffusion controlled) molybdenum in alloys [19].

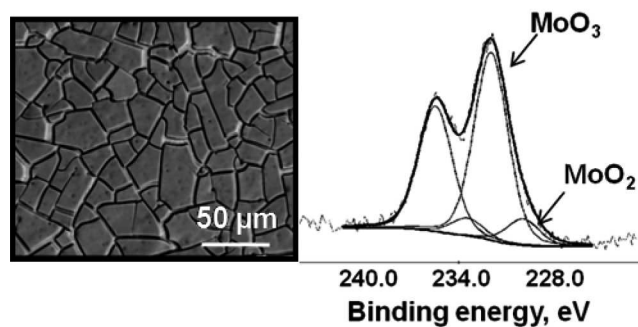


Fig. 5. SEM image of the deposit electroplated at  $-1.1\text{ V/SCE}$  and corresponding X-ray photoelectron spectrum of Mo 3d binding energy level

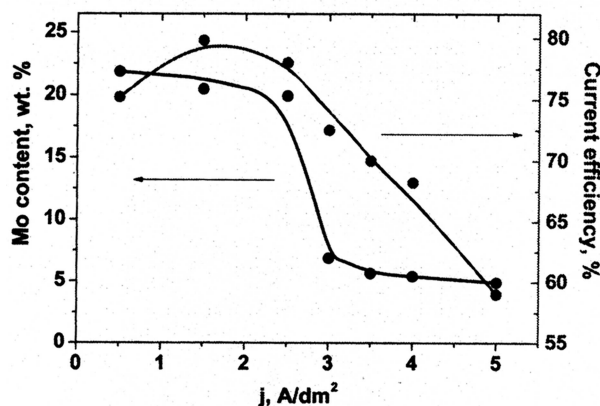


Fig. 6. Molybdenum content (wt. %) in Ni-Mo alloys and current efficiency of cathodic process as a function of the current density

The change in the chemical composition of Ni-Mo coatings (due to different current density values) is correlated with a significant change in their microstructures. This dependency corresponds to beneficial (regarding the mechanical properties) morphology changes from nodular to more compact and homogenous with a reduction of surface roughness for coatings deposited at current densities above  $3\text{ A/dm}^2$  (e.g.  $R_a = 0.27\text{ }\mu\text{m}$  and  $R_a = 0.18\text{ }\mu\text{m}$  for coating obtained at current density of  $2.5\text{ A/dm}^2$  and  $4\text{ A/dm}^2$ , respectively) (Fig. 7 and 8).

XRD analysis revealed that Ni-Mo alloys consist of a face-centred-cubic solid solution, what has been proved by the absence of peaks related to molybdenum in the diffractograms. Moreover, the line broadening with increase of molybdenum content and their gradual intensity decrease were observed (Fig. 9). The grain size was calculated using Rietveld algorithms in MAUD software [27]. The finest grains ( $\sim 5\text{ nm}$ ) were estimated for coatings with the highest molybdenum content ( $22.2\text{ wt.}\%$ ). For those alloys with less molybdenum content a slight increase of grain size up to a maximal value of about  $10\text{ nm}$  for alloy of  $4.9\text{ wt.}\%$  Mo has been obtained.

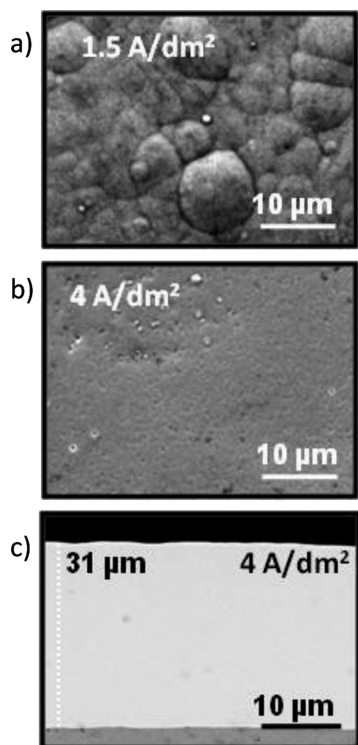


Fig. 7. SEM images of surface morphology of Ni-Mo coatings ( $\sim 10 \mu\text{m}$ ) electrodeposited at current density: a)  $2.5 \text{ A/dm}^2$  ( $R_a = 0.27 \mu\text{m}$ ) and b)  $4 \text{ A/dm}^2$  ( $R_a = 0.18 \mu\text{m}$ ) and cross-section of coatings obtained at  $4 \text{ A/dm}^2$  c)

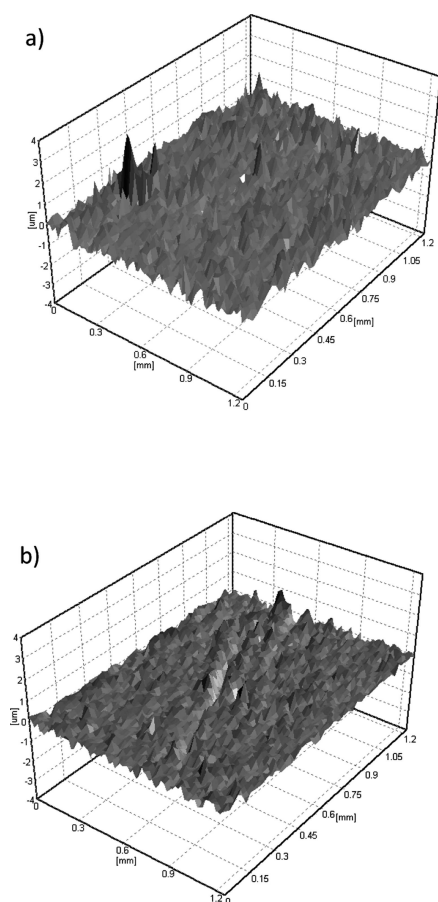


Fig. 8. 3D surface profile of Ni-Mo coatings deposited at different current densities: a)  $2.5 \text{ A/dm}^2$  ( $R_a = 0.27 \mu\text{m}$ ) and b)  $4 \text{ A/dm}^2$  ( $R_a = 0.18 \mu\text{m}$ )

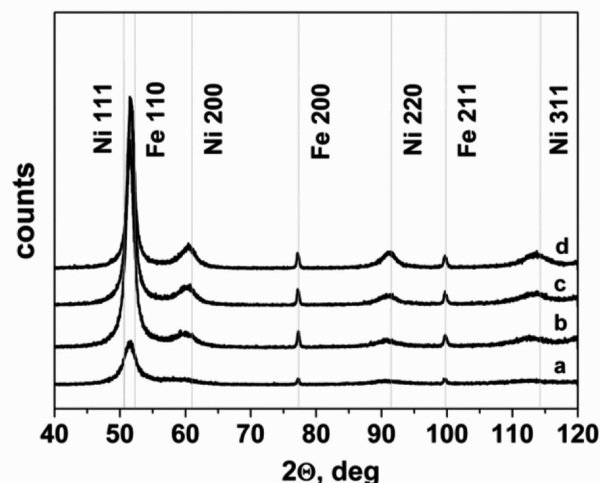


Fig. 9. X-ray diffraction patterns of Ni-Mo alloys electrodeposited at current density: a)  $1.5 \text{ A/dm}^2$  (22.2 wt.% Mo), b)  $2.5 \text{ A/dm}^2$  (19.0 wt.% Mo), c)  $4 \text{ A/dm}^2$  (5.4 wt.% Mo) and d)  $5 \text{ A/dm}^2$  (4.9 wt.% Mo)

The corrosion behavior of selected Ni-Mo coatings (electrodeposited at  $4 \text{ A/dm}^2$ ) as well as Cr coatings (WSK PZL Rzeszow) and steel substrate (S235JR), analyzed in  $0.5\text{M NaCl}$  and  $0.5\text{M Na}_2\text{SO}_4$  solutions, are shown in Fig.10 and Fig. 11, respectively. The corrosion properties are summarized in TABLE 1.

TABLE 1  
Corrosion properties ( $E_{corr}$ , mV – corrosion potential,  $i_{corr}$ ,  $\text{A/cm}^2$  – corrosion current density) of Ni-Mo, Cr and steel substrate (S235JR) in  $0.5\text{M NaCl}$  and  $0.5\text{M Na}_2\text{SO}_4$  solutions

Sample	0.5M NaCl		0.5M Na <sub>2</sub> SO <sub>4</sub>	
	$E_{corr}$ vs. Ag/AgCl, mV	$i_{corr}$ , $\text{A/cm}^2$	$E_{corr}$ vs. Ag/AgCl, mV	$i_{corr}$ , $\text{A/cm}^2$
Ni-Mo	-0.523	$3.7 \cdot 10^{-6}$	-0.580	$1.52 \cdot 10^{-6}$
Cr	-0.402	$8.09 \cdot 10^{-8}$	-0.513	$1.17 \cdot 10^{-6}$
S235JR	-0.649	$1.69 \cdot 10^{-5}$	-0.674	$4.20 \cdot 10^{-6}$

As seen, chromium coating has the most positive corrosion potential in both investigated corrosion environments. In the same conditions Ni-Mo deposits are characterized by more negative corrosion potential and higher corrosion current, than chromium coatings. However, for both coatings the monotonic increase of the anodic current density in  $0.5 \text{ M NaCl}$  is associated with the uniform dissolution of samples. In  $0.5\text{M Na}_2\text{SO}_4$  solutions Ni-Mo deposit has similar corrosion properties (corrosion potential, corrosion current density) to chromium coating. Furthermore, in the potential range from  $+0.28\text{V}$  to  $+1\text{V}$  for Ni-Mo and to  $+0.72\text{V}$  for chromium coatings in the polarization curve a current plateau is visible. It is correlated with the formation of surface films, which can block dissolution of the coatings. As expected for steel samples, in NaCl as well as in  $\text{Na}_2\text{SO}_4$  solutions the more negative corrosion potential and the highest corrosion current were observed.

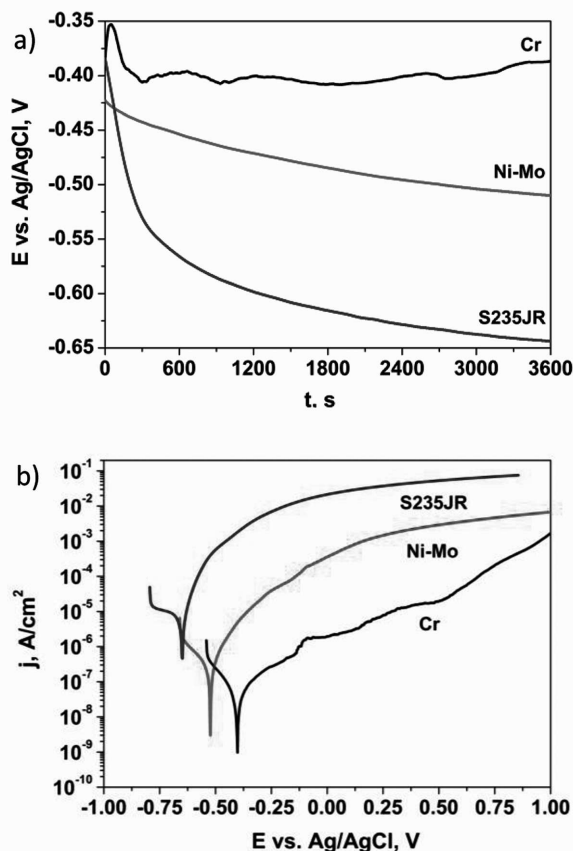


Fig. 10. a) Corrosion potential vs. Ag/AgCl reference electrode as a function of time, b) polarization curves of Ni-Mo, Cr and steel substrate (S235JR) in 0.5M NaCl

Microindentation tests revealed that all deposits are characterized by a relatively good microhardness which varied from 6.6 to 7.8 GPa and Young's modulus value from 180 to 250 GPa (TABLE 2).

Significant increase in the wear and friction resistance of coatings with increase of the current density of the electrodeposition process has been observed. The depth of wear scar was small compared with coatings thickness (~10  $\mu\text{m}$ ) for all analyzed deposits. Nevertheless, wear rate ( $W_v$ ) calculated as a ratio of the worn volume to the applied load on sliding distance as well as friction coefficient were much lower for coatings obtained above 3 A/dm<sup>2</sup> (Fig. 12, TABLE 2). This effect is mainly influenced by a decrease of surface roughness and changes to a more compact and uniform morphology of the deposit.

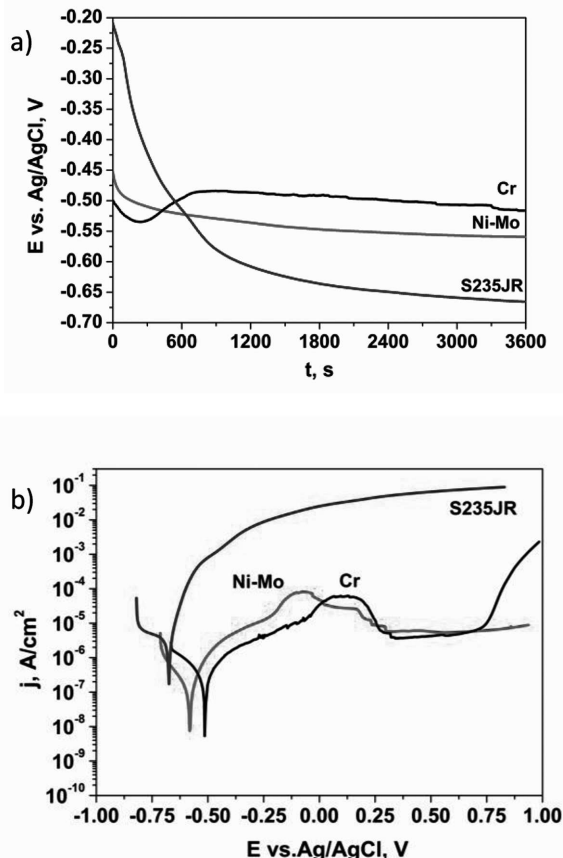


Fig. 11. a) Corrosion potential vs. Ag/AgCl reference electrode as a function of time, b) polarization curves of Ni-Mo, Cr and steel substrate (S235JR) in 0.5M Na<sub>2</sub>SO<sub>4</sub>

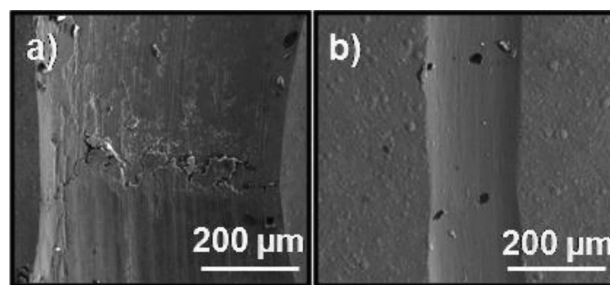


Fig. 12. SEM images of surface of Ni-Mo coatings electrodeposited at current density: a) 1.5 A/dm<sup>2</sup> and b) 5 A/dm<sup>2</sup> after a ball-on-disk test

TABLE 2

Properties of Ni-Mo coatings deposited at different current density ( $j$ , A/dm<sup>2</sup>) (Mo, wt.% – molybdenum content;  $H_{IT}$ , GPa – indentation microhardness;  $E_{IT}$ , GPa – Young's modulus)

$j$ , A/dm <sup>2</sup>	Mo, wt. %	$H_{IT}$ , GPa	$E_{IT}$ , GPa	Wear coefficient, 10 <sup>-6</sup> mm <sup>3</sup> /Nm	Friction coefficient	Critical load, N
0.5	22.2±0.4	6.6±0.3	184±14	823±47	0.85	>30
1.5	21.0±0.4	7.6±0.4	188±12	965±94	0.85	>30
3	6.9±0.3	7.6±0.3	201±16	18±3	0.30	18
4	5.4±0.5	7.4±0.4	182±15	8±2	0.24	>30
5	4.9±0.5	6.7±0.2	181±12	17±3	0.23	>30

The adhesion of coatings to the steel substrate and deformation mechanism under increasing load were determined by microscratch test. For coatings obtained in the region of lower current density ( $j < 3 \text{ A/dm}^2$ ) only plastic deformation and no cracks and delamination up to maximum load of 30N were observed. For stiffer coatings deposited at  $3 \text{ A/dm}^2$ , which were characterized by the highest Young's modulus, first cohesive cracks appeared when the load exceeded 18N. With further increase of current density of the electrodeposition process coatings again were characterized by plastic deformation similar to that of coatings obtained at lower current density. However, in this case also enhanced wear and friction resistance was observed.

#### 4. Conclusions

From the specially designed citrate bath with the selected operating conditions metallic, homogenous and well adherent to the steel substrate Ni-Mo alloys were obtained. The pH of bath causes significant surface quality changes of the coatings, which become more compact and crack-free at pH above 8. Moreover, the increase of the applied current density causes a reduction of the molybdenum content in alloys, what corresponds to modification of deposit morphology from globular to more uniform, reduction in roughness and the slightly increase of the average crystallite size (up to a maximum value of about 10 nm). Consequently, coatings electrodeposited at current densities above  $3.5 \text{ A/dm}^2$  are characterized by the most promising micromechanical and tribological properties: high microhardness, excellence wear (50-100 times lower wear index than for coatings obtained below  $3.5 \text{ A/dm}^2$ ) and friction resistance. Furthermore, Ni-Mo alloys exhibit similar anticorrosive properties to chromium coating determined in sodium sulphate solution, but worst than the ones obtained in chloride environment.

#### Acknowledgements

The results presented in this paper were supported by the National Science Centre in the frame of the project no. 2011/01/B/ST8/03974 and within the project "KomCerMet" no. POIG.01.03.01-14-013/08-00 with the Polish Ministry of Science and Higher Education in the framework of the Operational Programme Innovative Economy 2007-2013.

#### REFERENCES

[1] E.W. Brooman, *Met. Finish.* **98**, 42 (2000).

- [2] W.Z. Friend, *Corrosion of Nickel and Nickel-base Alloys*, New York 1980.
- [3] C.C. Hu, C.Y. Weng, *J. Appl. Electrochem.* **30**, 499 (2000).
- [4] J.F. Kriz, H. Shimada, Y. Yoshimura, N. Matsubayashi, A. Nishijima, *Fuel* **74**, 1852 (1995).
- [5] M.P. Astier, G. Dij, S.J. Teichner, *Appl.Catal.* **72**, 321 (1991).
- [6] L.S. Sanches, S.H. Domingue, C.E.B. Marino, L.H. Mascaro, *Electrochem Commun.* **6**, 543 (2004)
- [7] M. Donten, H. Cesiulis, Z. Stojek, *Electrochim. Acta* **50**, 1405 (2005).
- [8] E. Chassaing, N. Portail, A.F. Levy, G. Wang, *J. Appl. Electrochem.* **34**, 1085 (2004).
- [9] E. Beltowska-Lehman, A. Bigos, P. Indyka, M. Kot, *Surf Coat Tech.* **211**, 67 (2011).
- [10] A. Brenner, *Electrodeposition of Alloys*, Vol. 1, New York, London 1963.
- [11] T. Akiyama, H. Fukushima, *Iron Steel Inst. Jpn.* **32**, 787 (1992).
- [12] E.J. Podlaha, D. Landolt, *J. Electrochem. Soc.* **43**, 885 (1996).
- [13] E.J. Podlaha, D. Landolt, *J. Electrochem. Soc.* **43**, 893 (1996).
- [14] H. Fukusima, T. Akiyama, S. Akagi, K. Higashi, *Trans. Jpn. Inst. Met.* **20**, 358 (1979).
- [15] E. Chassaing, K. Yu Quang, R. Wiart, *J. Appl. Electrochem.* **19**, 839 (1989).
- [16] E. Beltowska-Lehman, E. Chassaing, K. Vu Quang, **21**, 606 (1991).
- [17] T. Murase, M. Ogawa, T. Hirato, Y. Awakura, *J. Electrochem. Soc.* **151**, C798 (2004).
- [18] M. Pushpavanam, K. Balakrishnan, *J. Appl. Electrochem.* **26**, 1065 (1996).
- [19] E. Beltowska-Lehman, P. Indyka, *Thin Solid Films* **520**, 2046 (2012).
- [20] P. Indyka, E. Beltowska-Lehman, M. Faryna, K. Berent, A. Rakowska, *Arch. Metall.* **55**, 421 (2010).
- [21] L. Alderighi, P. Gans, A. Ienco, D. Peters, A. Sabatini, A. Vacca, *Cordin Chem Rev.* **184**, 311 (1999).
- [22] J.J. Cruywagen, E.A. Rohwer, G.F.S. Wessels, *Polyhedron* **14**, 3481 (1995).
- [23] M. Ishikawa, H. Enomoto, C. Iwakura, *Electrochim. Acta* **39**, 2153 (1994).
- [24] E. Beltowska-Lehman, *Phys. Stat. Sol.* **5**, 3514 (2008).
- [25] K. Hashimoto, T. Sasaki, S. Meguro, K. Asami, *Mater. Sci. Eng.* **942**, 375 (2004).
- [26] J. Halim, R. Adbel-Karim, S. El-Raghy, M. Nabil, A. Waheed, *J. Nanomater.* (2012) DOI: 10.1155/2012/845673 (in press).
- [27] L. Lutterotti, P. Scardi, *J. Appl. Crys.* **23**, 246 (1990).